ISSN (Print) : 0974-6846
ISSN (Online) : 0974-5645
Indian Journal of Science and Technology, *Vol 8(10), 906–912, May 2015* DOI: 10.17485/ijst/2015/v8i10/53596

Coherent Response of a Human Eye: An Apodization Model of Stiles Crawford Effect of the First Kind

Nachieketa K. Sharma*

Department of Physics, Institute of Technical Education and Research, Siksha 'O' Anusandhan University, Bhubaneswar-751030, Odisha, India; nachiketasharma@soauniversity.ac.in

Abstract

In Stiles Crawford effect of the first kind a beam entering a pupil from the edge shows a diminution in the effective brightness compared to an identical beam passing axially. The same reduction in brightness is also observed in a pupil becoming gradually less transparent from the centre toward its periphery, known as pupil apodization. In this study we have treated Stiles Crawford effect as pupil apodization and evaluated the modulation in the retinal image using a periodic object of infinite cycles with a saw-tooth wave transmission profile, both under incoherent and coherent illumination. Over a wide range of spatial frequencies, though the incoherent entering beam shows a gradual decrease in the modification, no change is observed for coherent illumination. Thus, the modeling of Stiles Crawford effect as pupil apodization is insensitive to coherent illumination and the retinal distribution of light is dependent on the coherence of the incident beam apart from pupil entry point of the beam in traditional Stiles Crawford effect. Hence, this study highlights the significance of employing coherence in the entering beam as an optical parameter in governing retinal response and understanding the spatial distribution of photon absorption in the photoreceptors of a human eye.

Keywords: Apodization, Coherent Illumination, Modulation, Saw-Tooth Wave, Stiles-Crawford Effect

1. Introduction

A beam of light stimulates the retina weakly when its entry to the pupil is gradually shifted from the centre toward the edge. This is manifested as a reduction in visibility, also known as Stiles-Crawford effect of the first kind (SCE I)[1]. The same kind of reduction in brightness in an image is also observed when the pupil allowing the light to enter is covered with a filter which becomes less and less transparent from the centre toward the edge[2]. This is known as apodization. Due to this outward resemblance between the retinal Stiles-Crawford effect and pupil apodization, the SCE I has been modeled as a pupil apodization in studying retinal light distributions in many imaging situations[3–6]. And this approach of treating SCE I as pupil apodization is justified as light is assumed to enter into the receptor through a single accepting aperture[7].

Mathematically, SCE I is expressed either as $\eta = 10^{-\rho_{10} r^2}$ or $\eta = e^{-\rho_e r^2}$, where r is the distance in the entrance pupil from the origin of the function and η is the visibility[8]. The coefficients (of directionality that measures the width of the pupil apodization) ρ_e and ρ_{10} are related by $\rho_e = \ln 10 \rho_{10} = 2.3\rho_{10}$. In the absence of aberrations, both the approaches, of modeling the Stiles-Crawford effect of the first kind as pupil apodization and the waveguiding of light in the photoreceptors give identical predictions for effective retinal light distributions[9–13].

The extensive literature available for modulation evaluation studies has made use of various test targets under incoherent illumination[14–20]. But no work appears to have been done which simultaneously combine all the three parameters of 1. Treating the SCE I as a pupil apodization, 2. Choosing a test target of saw-tooth wave profile and 3. Using a spatially coherent entering beam to evaluate modulation[21,22]. This has the significance of knowing about the changes in retinal light spatial distribution as a result of pupil apodization due to a grating structure of triangular transmission profile.

*Author for correspondence

2. Analysis and Images of Periodic Saw-tooth Wave Targets

2.1 Analysis

The technique of coherent imaging involves the following stages: first, the amplitude of light coming from the triangular grating is spatially Fourier analyzed; next, it is filtered, and resynthesized as a distribution of amplitude of light in the retinal plane. At the end, the amplitude is squared to get retinal light distributions[23–25]. That is, an object with a complex amplitude distribution is Fourier transformed to produce its corresponding spatial frequency spectrum. The apodizer, here SCE I modifies the object spectrum and the modified object spectrum is then inverse Fourier transformed to get the image complex amplitude distribution. Finally, the squared modulus of this amplitude gives the intensity distribution in the image from which the modulation is computed to ascertain the changes in retinal light spatial distribution in coherent illumination.

2.2 Images of Periodic Saw-tooth Wave Targets

The transmission function of a periodic saw-tooth wave pattern can be mathematically defined as follows[26].

$$A(x) = h + m(x+b) \text{ for } 0 < x < a - b$$

$$= h + m(x + b - 2a) \text{ for } a - b < x < 2a.$$

Where h is the mean level of irradiance in the object, m is the slope of the pattern and 2a is the period for which the corresponding spatial frequency is $\omega = \frac{\pi}{a}$.

The Fourier series representation of the above object transmission function is given by:[26,27]

$$A(x,y) = h - \sum_{n=1}^{\infty} \frac{2am}{n\pi} \cos(n\pi) \sin(n\omega x) \quad (1)$$

where $\omega = \frac{2\pi}{2a} = \frac{\pi}{a}$ and x, y are the horizontal and vertical coordinates of space.

The Fourier transform of Equation (1) leads to

$$a(u,v) = \int_{-\infty}^{\infty}\int A(x,y) e^{-i(ux+vy)} dxdy$$

$$= \int_{-\infty}^{\infty}\int \left[h - \sum_{n=1}^{\infty} \frac{2am}{n\pi} \cos(n\pi) \sin(n\omega x) \right] e^{-i(ux+vy)} dxdy \quad (2)$$

The evaluation of the above integral calls for the use of the two dimensional Dirac delta function defined as

$$\delta(p,r) = \int_{-\infty}^{\infty}\int e^{-i(pq+rs)} dqds \quad (3)$$

For simplicity of mathematical steps

Let $K_n = \frac{2am}{n\pi} \cos(n\pi)$

Thus Eq. (2) reduces to

$$a(u,v) = \int_{-\infty}^{\infty}\int \left[h - \sum_{n=1}^{\infty} K_n \sin(n\omega x) \right] e^{-i(ux+vy)} dxdy$$

$$= h \int_{-\infty}^{\infty}\int e^{-i(ux+vy)} dxdy + \sum_{n=1}^{\infty} K_n \int_{-\infty}^{\infty}\int \sin(n\omega x) e^{-i(ux+vy)} dxdy$$

$$= h\delta(u,x) - \sum_{n=1}^{\infty} \frac{K_n}{2i} \int_{-\infty}^{\infty}\int \left[e^{-i[(u-n\omega)x+vy]} - e^{-i[(u+n\omega)x+vy]} \right] dxdy$$

$$= h\delta(u,v) - \frac{1}{2i} \sum_{n=1}^{\infty} K_n \left[\delta(u-n\omega, v) - \delta(u+n\omega, v) \right]$$

Given that the Fourier transform of the input to the pupil is $a(u,v)$, pupil exit function will be $f(u,v)a(u,v) = a'(u,v)$ for f being the amplitude transfer function which we approximate as follows[28]:

$$f(u,v) = \begin{cases} e^{\frac{-(u^2+v^2)}{\sigma^2}} & \text{if } u^2+v^2 < K, \\ 0 & otherwise \end{cases}$$

where K = 1 for diffraction-limited coherent imaging systems, and K = 2 for diffraction -limited incoherent imaging systems[28,29–31] for apodization parameter σ = 3.086[8]

$$a'(u,v) = e^{\frac{-(u^2+v^2)}{\sigma^2}} \left[h\delta(u,v) - \frac{1}{2i} \sum_{n=1}^{\infty} K_n \left[\delta(u-n\omega, v) - \delta(u+n\omega, v) \right] \right] \quad (4)$$

The image amplitude distribution at the exit pupil is obtained by the inverse Fourier transform of the spectrum $a'(u,v)$. Thus

$$A'(x,y) = \int_{-\infty}^{\infty}\int a'(u,v) e^{i(ux+vy)} dudv$$

$$A'(x,y)=\int_{-\infty}^{\infty}\int_{-\infty}^{\infty} f(u,v)\left[h\delta(u,v)-\frac{1}{2i}\sum_{n=1}^{\infty}K_n\left[\delta(u-n\omega,v)-\delta(u+n\omega,v)\right]\right]e^{i(ux+vy)}dudv$$

$$=h-\sum_{n=1}^{\infty}K_n\int_{-\infty}^{\infty}\int_{-\infty}^{\infty}\frac{\left[\delta(u-n\omega,v)-\delta(u+n\omega,v)\right]}{2i}f(u,v)e^{i(ux+vy)}dudv$$

$$=h-\sum_{-\infty}^{\infty}K_n f(n\omega,0)\sin(n\omega x)$$

Substituting back in for K_n yields

$$A'(x,y)=h-\sum_{n=1}^{\infty}\frac{2am}{n\pi}\cos(n\pi)f(n\omega,0)\sin(n\omega x) \quad (5)$$

As $f(n\omega,0)=0$ for $nw \geq 1$ the upper limit n' of n is such that $nw<1$. So, Equation (5) will be

$$A'(x,y)=h-\sum_{n=1}^{n'}\frac{2am}{n\pi}\cos(n\pi)f(n\omega,0)\sin(n\omega x) \quad (6)$$

Finally, the image energy distribution will be given by the squared modulus of above as

$$\left|A'(x,y)\right|^2=\left[h-\sum_{n=1}^{n'}\frac{2am}{n\pi}\cos(n\pi)e^{-0.105n^2\omega^2}\sin(n\omega x)\right]^2 \quad (7)$$

ωx can vary from 0 to π to compute maximum and minimum image energy distribution.

The modulation in the image (for unit contrast in the object) can be defined as

$$M=\frac{\left|A'(x,y)\right|^2_{max}-\left|A'(x,y)\right|^2_{min}}{\left|A'(x,y)\right|^2_{max}+\left|A'(x,y)\right|^2_{min}} \quad (8)$$

As the incoherent imaging is linear in image energy distribution, rather than amplitude the image energy distribution and the corresponding modulation equations for incoherent illumination will be given by

$$I(x,y)_{incohernt}=h-\sum_{n=1}^{n'}\frac{2am}{n\pi}\cos(n\pi)e^{-0.105n^2\omega^2}\sin(n\omega x) \quad (9)$$

As $f(n\omega,0)=0$ for $nw \geq 2$ the upper limit n' of n is such that $nw<2$ for incoherent illumination[28,29].

$$M_{inc.}=\frac{I_{max}-I_{min}}{I_{max}+I_{min}} \quad (10)$$

3. Result and Discussion

The retinal light distributions in the images of periodic saw-tooth wave targets, formed by a human eye with SCE-I modelled as pupil apodization under coherent and incoherent illumination was computed using Equation (7) and Equation (9) respectively. Equation (8) is used to find out the modulations in the images of saw-tooth wave grating targets for coherent illumination. Similarly modulation is evaluated for the incoherent illumination using Equation (10). The values are plotted from Figure 1 to Figure 3. The cut-off frequency is the highest spatial frequency that a normal human eye could resolve if it had perfect optics. So, the fineness of the retinal sampling array imposes a 75 Hz cut-off on sine waves that can be delivered to the retina using incoherent light. And for coherent light this will be lower, i.e., 37.5 cycles/deg[29–31]. All the computations are tabulated in Table 1 and 2.

1. From Figure 1, it is seen that the modification in the modulation registers a change limited to a mere 2% over the entire spatial frequency range for all possible values of the slope. Though to a minor extent the slope governs the modulation, the striking behaviour is the near constancy of the modulation over the entire spatial frequency range for coherent entering light regardless of the values of the slope. This shows that coherence of the entering beam has also a role to play in governing retinal light distributions in addition to the pupil entry point of the beam in traditional Stiles Crawford effect. This is experimentally validated by the absence of an integrated Stiles Crawford function for coherent light[32,33].

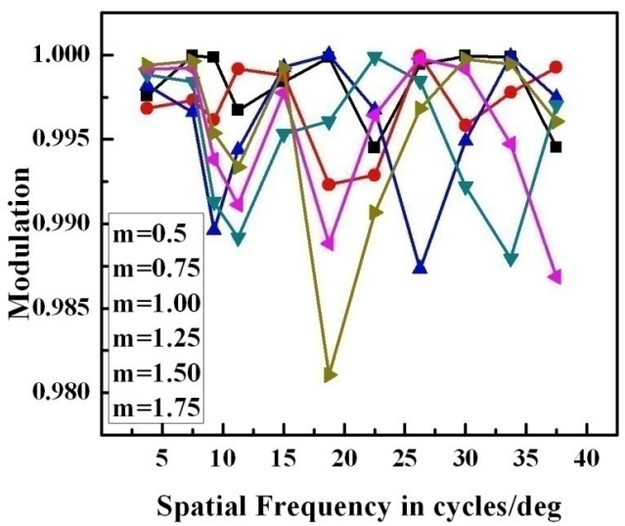

Figure 1. Modulation of a saw-tooth wave target for various slopes under coherent illumination. To a minor extent the slope governs the coherent response.

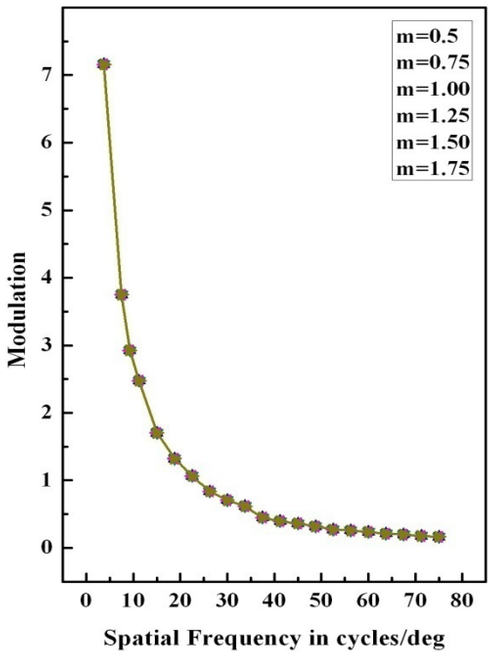

Figure 2. Modulation of a saw-tooth wave target for various slopes under incoherent illumination. The modulation behaves same regardless of the value of the slope.

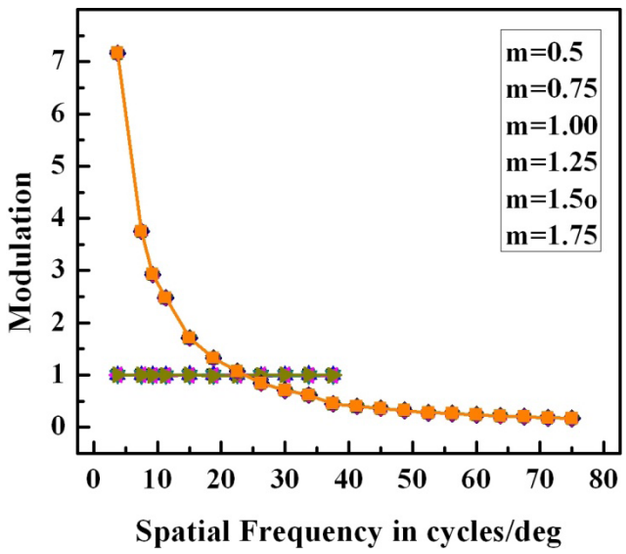

Figure 3. Modulation of a saw-tooth wave target for various slopes under both coherent and incoherent illumination. The straight line response is for coherent illumination.

2. σ = 3.086 is the value of the apodization parameter for a human eye with Stiles Crawford effect of the first kind[8]. This value is important for our study and we see from Figure 2 that when we incorporate this value in computing the modulation, the modulation falls gradually over the entire range of spatial frequencies in incoherent illumination[34]. That is, the incoherent response is only governed by Stiles Crawford effect.
3. The modulation under incoherent illumination keeps its behavior of decreasing with the increase in the value of the spatial frequency intact regardless of the value of the slope as ascertained from Table 2. That is, incoherent illumination responds favorably to spatial frequency and is insensitive to change of slope[34]. So, the incoherent response mimics the traditional Stiles Crawford effect.
4. Figure 3 depicts the overall response of modulation to spatial frequencies for apodization parameter 3.086 (a human eye with Stiles Crawford effect modeled as pupil apodization) both for coherent and incoherent light taken together. This figure clearly indicates that coherence in the entering beam (as modulation is quite different for incoherent illumination compared to the coherent one) has the potential to be used as an optical parameter in controlling retinal response[35].
5. Pupil apodization can be used as an optical technique to obtain retina light distributions in presence of Stiles-Crawford effect of the first kind regardless of the transmission profile of the test targets chosen[5,21].
6. The importance of Stiles-Crawford effect lies in the determination of the effective pupil apodization function for eye and vision modeling[36].
7. The modification the coherence in the entering beam causes to the Stiles Crawford visibility function can be employed as a bio-sensor in predicting the early onset of glaucoma.

4. Conclusion

Pupil apodization technique can be used to incorporate directional effects of the retina[5,10,20]. And the analysis of this directionality is needed to have a better understanding of the connection between the retinal image and the neural response since the retina plays a key role as the last optical element in the eye.

The modulation's inability in showing the expected modification in coherent illumination for a human eye where the SCE I is modeled as a pupil apodization points to a more deeper fact in working, that is, the retina prefers to respond to the more immediate stimulus of an interference pattern than to the pupil entry points of the entering beam hitherto governed traditionally by Stiles-Crawford

Table 1. Computation of Modulation for different apodization parameters over the entire range of spatial frequencies (ω) under coherent incident illumination

ω in c/deg	m = 0.5	m = 0.75	m = 1.0	m = 1.25	m = 1.5	m = 1.75
3.75	0.99758	0.99683	0.99818	0.99882	0.99917	0.99939
7.50	0.99994	0.99732	0.9966	0.99841	0.9992	0.99962
9.25	0.99984	0.99617	0.98961	0.99128	0.99381	0.99537
11.25	0.99672	0.99917	0.99436	0.98918	0.99113	0.99335
15.00	0.99841	0.99878	0.99927	0.99532	0.99776	0.99922
18.75	0.99985	0.99231	0.99999	0.99607	0.98884	0.98105
22.50	0.99449	0.99288	0.99673	0.99988	0.99642	0.99066
26.25	0.99944	0.99994	0.98732	0.99845	0.99977	0.99683
30.00	0.99994	0.99582	0.9949	0.99221	0.99916	0.99974
33.75	0.99989	0.99777	0.99992	0.98795	0.99474	0.99946
37.50	0.99451	0.99927	0.99747	0.99703	0.98686	0.99606

Table 2. Computation of Modulation for different apodization parameters over the entire range of spatial frequencies (ω) under incoherent incident illumination

ω in c/deg	m = 0.5	m = 0.75	m = 1.0	m = 1.25	m = 1.5	m = 1.75
3.75	7.1604	7.1604	7.1604	7.1604	7.1604	7.1604
7.50	3.75111	3.75111	3.75111	3.75111	3.75111	3.75111
9.25	2.92308	2.92308	2.92308	2.92308	2.92308	2.92308
11.25	2.47659	2.47659	2.47659	2.47659	2.47659	2.47659
15.00	1.70417	1.70417	1.70417	1.70417	1.70417	1.70417
18.75	1.32319	1.32319	1.32319	1.32319	1.32319	1.32319
22.50	1.06708	1.06708	1.06708	1.06708	1.06708	1.06708
26.25	0.83782	0.83782	0.83782	0.83782	0.83782	0.83782
30.00	0.70722	0.70722	0.70722	0.70722	0.70722	0.70722
33.75	0.61799	0.61799	0.61799	0.61799	0.61799	0.61799
37.50	0.45016	0.45016	0.45016	0.45016	0.45016	0.45016
41.25	0.39631	0.39631	0.39631	0.39631	0.39631	0.39631
45.00	0.36106	0.36106	0.36106	0.36106	0.36106	0.36106
48.75	0.31821	0.31821	0.31821	0.31821	0.31821	0.31821
52.50	0.27238	0.27238	0.27238	0.27238	0.27238	0.27238
56.25	0.26056	0.26056	0.26056	0.26056	0.26056	0.26056
60.00	0.23693	0.23693	0.23693	0.23693	0.23693	0.23693
63.75	0.21409	0.21409	0.21409	0.21409	0.21409	0.21409
67.50	0.19925	0.19925	0.19925	0.19925	0.19925	0.19925
71.25	0.17797	0.17797	0.17797	0.17797	0.17797	0.17797
75.00	0.16426	0.16426	0.16426	0.16426	0.16426	0.16426

effect of the first kind only. Recent experiments[5,32,33] have also validated such line of arguments and findings. Moreover, apodization as an optical technique can be successfully used to compute retinal response regardless of the profile of the test objects employed.

The significance of the work lies in the potentiality of coherence being used as an optical parameter in regulating retinal stimulation and understanding the spatial distribution of photon absorption in the photoreceptors of a human eye.

5. References

1. Stiles WS, Crawford BH. The luminous efficiency of rays entering the pupil at different points. Proc Roy Soc B. 1933 Mar; 112:428–50.
2. Jacquinot P, Bougron P, Dossier B. Calcul et realisation des distributions d'amplitude pupillaire, permettant a suppression des franges laterale dans les figures de diffraction. In: Fleury P Marechal A, Anglade C, editors. La Theorie des Images Optiques. Paris: Editions de la Revue d'Optique; 1949. p. 183–93.
3. Westheimer G. Retinal light distributions, the Stiles-Crawford effect and apodization. J Opt Soc Am A. 2013 Jul; 30:1417–21.
4. Metcalf H. Stiles-Crawford apodization. J Opt Soc Am. 1965; 55:72–3.
5. Sharma NK, Mishra K, Kamilla SK, Sharma JK. Using pupil apodization as an optical technique to obtain retina light distributions in presence of stiles-crawford effect of the first kind. International Journal of Microwave and Optical Technology. 2014 May; 9(3):259–66.
6. Atchison DA, Scott DH, Strang NC, Artal P. Influence of Stiles-Crawford effect apodization on visual acuity. J Opt Soc Am A. 2002; 19:1073–83.
7. Westheimer G. Specifying and controlling the optical image on the retina. Prog Retinal Eye Res. 2006 Jan; 25: 19–42.
8. Applegate RA, Lakshminarayanan V. Parametric representation of Stiles-Crawford functions: normal variation of peak location and directionality. J Opt Soc Am A. 1993; 10:1611–23.
9. Vohnsen B, Iglesias I, Artal P. Guided light and diffraction model of human-eye photoreceptors. J Opt Soc Am A. 2005; 22(11):2318–28.
10. Vohnsen B. Photoreceptor waveguides and effective retinal image quality. J Opt Soc Am A. 2007 Mar; 24(3):597–607.
11. Snyder AW, Pask C. The Stiles-Crawford effect-explanation and consequences. Vis Res. 1973; 13(6):1115–37.
12. Sharma NK, Mishra K, Kamilla SK, Sharma JK. Using Bacteriorhodopsin Thin Film in Regulating Retinal Stimulation of a Human Eye. Adv Sci Lett. 2014 Mar; 20(3–4):705–9.
13. Sharma NK, Mishra K, Kamilla SK, Sharma JK. Modelling of a retinal cone using erbium/ytterbium doped polymethylmethacrylate and crown glass. Adv Sci Lett. 2014 Mar; 20(3-4):788–91.
14. Hopkins HH. 21st Thomas Young Oration. The application of frequency response techniques in optics. Proc Phys Soc. 1962; 79:889–919.
15. Barakat R, Houston A. Modulation of square-wave objects in incoherent light. I J Opt Soc Am. 1963 Dec; 53(12): 1371–6.
16. Singh K, Chopra KN. Method of measuring the modulation transfer function of an apodized circular aperture. J Opt Soc Am. 1963; 60:641–5.
17. Katti PK, Singh K, Kavathekar AK. Effect of an apodizing screen on the rectangular and triangular wave response of a circular aperture with incoherent incident light. Appl Opt. 1970; 9:129–33.
18. Katti PK, Singh K, Kavathekar AK. Modulation of a general periodic object with triangular transmission profile by an annular aperture using incident incohe rent light. Optica Acta. 1969; 16:629–39.
19. Jaiswal AK, Bhogra RK. Performance of apodized apertures under partially coherent illumination. Opt Acta. 1973; 20:965–77.
20. Atchison DA, Joblin A, Smith G. Influence of Stiles–Crawford effect apodization on spatial visual performance. J Opt Soc Am A. 1998 Sep; 15: 2545–51.
21. Sharma NK, Mishra K, Kamilla SK, Sharma JK. Performance of a human eye in coherent illumination. 2013 Workshop on Recent Advances in Photonics (WRAP); IEEE Xplore; 2013 Dec 17–18. p.1–2.
22. Sharma, NK, Mishra K, Kamilla SK. Modulation of a periodic object with infinitely thin lines by a human eye in presence of Stiles-Crawford Effect of the first kind using coherent light. Orissa Journal of Physics. 2014; 21(1):57–64.
23. Westheimer G. Retinal light distribution for circular apertures in Maxwellian View. J Opt Soc Am. 1959; 49: 41–9.
24. Hopkins HH. The numerical evaluation of the frequency response of optical systems. Proc Phys Soc B. 1957; 70:1002.
25. Born M, Wolf E. Principles of Optics. 7th ed. Reissued by Cambridge University Press ; 1997.
26. Deb KK, Mondal PK, Atti Fond G. Ronchi. 1974; 29:741.
27. van Meeteren A. Calculations on the optical modulation function of the human eye for white light. Opt Acta. 1972; 21:395–412.
28. Goodman JW. Introduction to Fourier Optics. 3rd ed. Viva Books; 2007.

29. Smith W. Modern Optical Engineering. 4th ed. McGraw-Hill Professional; 2007.
30. Applegate RA. Limits to Vision: Can We Do Better Than Nature. J Refract Surg. 2000; 16.
31. Boreman GD. Modulation transfer function in optical and electro-optical systems. Bellingham, WA: SPIE Press; 2001.
32. Vohnsen B, Rativa D. Absence of an integrated Stiles-Crawford function for coherent Light. J Vis. 2011; 11(1):1–10.
33. Castillo S, Vohnsen B. Exploring the SCE-I with coherent light and dual Maxwellian Sources. Applied Optics. 2013; 52:A1–8.
34. Ghosh S. Studies on incoherent image formation of periodic objects by a human eye in the presence of Stiles Crawford effect of the fist kind [PhD Thesis]. Hyderabad, India: Osmania University; 2009.
35. Westheimer G. Directional sensitivity of the retina: 75 years of Stiles-Crawford effect. Proc Roy Soc B. 2008; 275: 2777–86.
36. Vohnsen B, Lochocki B, Vela C. Integrated Stiles-Crawford effect in normal vision. In: Iskander DR, Kasprzak HT, editors. Proceedings VII European/I World Meeting in Visual and Physiological Optics. Wroclaw, Poland; 2014 Aug 25-27.